



# *Ab initio* MCDHF/RCI calculations of mass- and field shifts isotopes parameters of the $1s^2 \ ^1S_0 - 1s \ 2p \ ^1P_1^o$ and $1s^2 \ ^1S_0 - 1s \ 2p \ ^3P_{0,1,2}^o$ transitions in He-like ions for the sequence $2 \leq Z \leq 83$

Sirine Ben Nasr<sup>a</sup>, Soumaya Manai<sup>b,d</sup>, Dhia Elhak Salhi<sup>b,c</sup>, Haikel Jelassi<sup>b,\*</sup>

<sup>a</sup> Physique Atomique et Astrophysique, Université de Mons, B-7000 Mons, Belgium

<sup>b</sup> Laboratory on Energy and Matter for Nuclear Sciences Development, LR16CNSTN02, Tunisia. National Center for Nuclear Sciences and Technologies, Sidi Thabet Technopark 2020 Ariana, Tunisia

<sup>c</sup> Faculty of Sciences of Tunis, University Tunis El Manar Tunis, Tunisia

<sup>d</sup> Faculty of Sciences of Bizerte, University of Carthage, Tunisia

## ARTICLE INFO

### Keywords:

Multiconfiguration Dirac–Hartree–Fock  
Mass shift  
Field shift  
Isotope shift

## ABSTRACT

Based on the multiconfiguration Dirac–Hartree–Fock method, the field shift and mass shift parameters of the  $1s^2 \ ^1S_0 - 1s \ 2p \ ^1P_1^o$  and  $1s^2 \ ^1S_0 - 1s \ 2p \ ^3P_{0,1,2}^o$  transitions in He-like ions for the sequence  $2 \leq Z \leq 83$  are calculated with high precision. The total value of the isotope shift is determined by the sum of the mass- and field-shifts. With the inclusion of the Breit interaction and the leading QED corrections, we find that the mass shift parameters of these transitions do not change monotonously along the isoelectronic sequence in the high-Z range due to the relativistic nuclear recoil effects. In addition, the field shifts and mass shifts of these four transitions are estimated and compared along the isoelectronic sequence.

## 1. Introduction

Isotope shift (IS) measurements are known as an important source for information about changes in the nuclear charge radii and distributions. Adding a number of neutrons makes the nuclei heavier and modify its charge distribution [1,2]. Also, measurements became possible for long sequences of stable and radioactive isotopes by optical laser spectroscopy [3]. This latter provides nuclear-model-independent data when the electronic part of the isotope shifts is well known. The atomic isotope shift parameters are important to analyze high-resolution solar and stellar spectra and understand nucleosynthesis mechanisms [4–6]. It is also necessary to include isotope shifts in modeling of spectra. Nevertheless, the use of *ab initio* calculations to determine the electronic parameters is important in view of the high sensitivity of the IS parameters to electronic correlation [7–9]. Due to up-to-date theoretical methods, we obtain more precise results for the electronic parameters. The isotope shift is composed of the field shift (FS) and mass shift (MS). For highly charged ions, the mass shift parameters makes a tiny contribution to the isotope shift but are not negligible. In theory, to achieve high accuracy the effects of electron correlations should be taken into account. In fact, many works carried out the isotope shift parameters of the low-lying states in highly charged ions such as H-like [10], He-like [11], Li-like [12] and B-like [13]. They found that the relativistic nuclear recoil corrections

contributes to the mass shifts for heavy elements. In fact, Zubova et al. carried out of some He-like ions  $Z = 12, 20, 30, 40, 50, 60, 70, 80, 90$  and 92 in their work [11].

This work aims to determine the electronic parameters relevant to the isotope shift for the four  $1s^2 \ ^1S_0 - 1s \ 2p \ ^1P_1^o$  and  $1s^2 \ ^1S_0 - 1s \ 2p \ ^3P_{0,1,2}^o$  transitions in He-like ions in the range from  $Z = 2$  to  $Z = 83$ . The electron correlation and Breit interaction are treated with the multiconfiguration Dirac–Hartree–Fock (MCDHF) method [14]. After obtaining the mass- and field-shifts of these transitions, we discussed the balance between this two parameters along the isoelectronic sequence with the assistance of the empirical formulas for the nuclear mass number and the nuclear mean-square radius. We describe our computational procedure, where the atomic state function is refined through a restricted active set approach using MCDHF/RCI computations from a multireference set of configuration state functions. Then, we summarize the energy level differences obtained with MCDHF/RCI computations through GRASP2018 code [15], normal- and specific-mass shifts resulting from the RIS4 module [16] implemented in GRASP2K [17]. Then, we give a detailed account of the mass and field shift parameters that are evaluated with RIS4 and the calculated atomic state functions.

\* Corresponding author.

E-mail addresses: [haikel.jelassi@cnstrn.rnrt.tn](mailto:haikel.jelassi@cnstrn.rnrt.tn), [haikel.jelassi@gmail.com](mailto:haikel.jelassi@gmail.com) (H. Jelassi).

## 2. Theory and calculations

### 2.1. MCDHF/RCI method

In the present work, we have adopted the GRASP2018 code developed by C. Froese Fischer et al. [15]. This code is fully relativistic and presents the new version of GRASP2K [17]. Like GRASP2K, GRASP2018 is based on the  $jj$ -coupling scheme and is used to obtain approximate wavefunctions describing the atomic levels. Our calculations are performed using the relativistic MCDHF method [14], implemented in GRASP2018 package [15]. For a many-electrons system, we take into account the Dirac–Coulomb hamiltonian given by:

$$H_{DC} = \sum_{i=1}^N (c\alpha_i \cdot \mathbf{p}_i + (\beta_i - 1)c^2 + V(r_i)) + \sum_{i>j} \frac{1}{r_{ij}}, \quad (1)$$

where  $V(r_i)$  is the mono-pole part of the electron–nucleus Coulomb interaction, in other terms it represents the Coulomb potential at radius  $r$ ,  $\alpha$  and  $\beta$  are the  $4 \times 4$  Dirac matrices,  $\mathbf{p}_i$  is the momentum operator of the electron  $i$  and  $c$  is the speed of light in atomic units. The first term describes electron kinetic energy and electron–nucleus interaction, the second term is the two-body Coulomb interactions between electrons. In multiconfiguration calculations the wave function for an atomic state is approximated by an atomic state function (ASF). The ASFs describing different fine structure levels are given as an expansion over configuration state functions (CSFs).

$$\psi(\gamma PJM) = \sum_{j=1}^{N_{CSF}} c_j \Phi(\gamma_j PJM) \quad (2)$$

where  $c_j$  are the mixing coefficients for the configuration  $j$ ,  $J$  and  $M$  are the angular quantum numbers and  $P$  is the parity. The label  $\gamma_j$  denotes appropriate information about the configuration state function  $j$ , such as parity, orbital occupancy and angular coupling scheme.

The CSFs are given as coupled anti-symmetric products of single-electron Dirac spinors. Based on a weighted energy functional of several states known as the extended optimal level (EOL) mode, where optimization is on a weighted sum of energies [18]. By applying the variational principle the radial parts of the Dirac orbitals are optimized to self-consistency in the relativistic self-consistent field (RSCF) procedure. Once a set of radial orbitals have been obtained, we used them to determine the mixing coefficients  $c_j$  of the multiconfiguration expansion of the CSFs by diagonalizing the Hamiltonian matrix.

It should be emphasized that instead of a pointlike nucleus, a finite nuclear charge distribution model—for instance, a uniform spherical model or a two-parameter Fermi model—must be used to generate the nuclear potential in the calculation in order to ensure the first-order perturbation to be valid for the field shift [19]. In the present work, the two-parameter Fermi nuclear model is adopted.

$$\rho = \frac{\rho_0}{1 + e^{(r-c)/a}} \quad (3)$$

Here  $\rho_0$  is a normalization coefficient,  $c$  is the half-density radius, and  $a = \frac{t}{4ln^3}$  is related to the surface thickness  $t$  of the charge distribution. In practice, the  $t = 2.30$  fm value is used and  $c$  is computed according to the formulas given in Ref. [19]. Since the ASFs are insensitive with respect to details of the nuclear model [20], the nuclear parameters from any stable isotope can be chosen to perform the SCF and RCI calculations.

### 2.2. Isotopic shift

The energy of a spectral line depends slightly on the isotope. Energy differences between isotopes are called isotope shifts. On the one hand, the angular momentum of an energy level has a definite fixed value, so if the mass of the atomic nucleus is changed, by substituting one isotope for another, the energy of the level will change so that the angular momentum remains the same. This change in energy is called a

mass shift (MS), or recoil effect and is the first major part of the isotope shift. Additionally, the nuclear charge distribution gives an electric field which determines the energy of the atomic electrons. A change in the energy of a level arising from a difference in this field between isotopes is called a field shift (FS). As a result, the total isotope shift can be obtained by the sum of these two effects,

$$IS = MS + FS. \quad (4)$$

The field shift is also called the volume shift. However, the term “field” is more appropriate since both the changes in shape and size of the nuclear charge distribution may lead to isotope shifts. The field shift is given in the approximation of the first-order perturbation theory by [19,21],

$$\Delta E_{FS}^{A,A'} = \langle \Psi(PJM) | \sum_i \delta V_i^{N,AA'} | \Psi(PJM) \rangle. \quad (5)$$

Here,  $\delta V^{N,AA'} = V^{N,A} - V^{N,A'}$  and the nuclear potential  $V^N$  for each isotope is produced by a two-parameter Fermi nuclear model [20,22]. Neglecting the higher-order nuclear moments [23], Eq. (5) is further simplified to,

$$\Delta E_{FS}^{A,A'} = F \delta \langle r^2 \rangle^{A,A'}, \quad (6)$$

where

$$F_k = \frac{2\pi}{3} \left( \frac{Ze^2}{4\pi\epsilon_0} \right) \Delta |\Psi(\mathbf{0})|_k^2 \quad (7)$$

is the field-shift factor proportional to the total electron probability density at the origin between the levels  $l$  and  $u$ ,

$$\Delta |\Psi(\mathbf{0})|_k^2 = \Delta \rho_k^e(0) = \rho_u^e(0) - \rho_l^e(0) \quad (8)$$

and  $\delta \langle r^2 \rangle^{A,A'}$  is the difference of the nuclear charge mean square radius between these two isotopes.

$$\delta \langle r^2 \rangle^{A,A'} = \langle r^2 \rangle^A - \langle r^2 \rangle^{A'} \quad (9)$$

Taking into account  $A' = A + 1$  in our approach. To evaluate the mass and the field shifts of the  $1s^2 {}^1S_0 - 1s 2p {}^3P_{0,2}^o$  and the  $1s^2 {}^1S_0 - 1s 2p {}^3P_1^o$  transitions for He-like ions, the difference of the nuclear mass and the mean-square charge radius for a given isotope pair should be determined. For convenience, we use the mass number  $A$  instead of the nuclear mass and adopt the empirical formula [24]:

$$Z = \frac{A}{1.98 + 0.015A^{2/3}}, \quad (10)$$

to inversely deduce  $A$  for a stable isotope of given atom with the atomic number  $Z$ . Considering two isotopes of the selected element, the difference of the nuclear charge mean square radius between these two isotopes  $\delta \langle r^2 \rangle^{A,A'}$  can be obtained via the empirical formula of mean square radius (in fm) [25] :

$$\langle r^2 \rangle^{1/2} = 0.836A^{1/3} + 0.570, (A > 9) \quad (11)$$

The mass shift between two isotopes  $A$  and  $A'$  caused by the motion of a nucleus with a finite mass is expressed as [26,27]

$$\Delta E_{MS}^{A,A'} = \frac{M' - M}{MM'} K_{MS}. \quad (12)$$

Here,  $M$  and  $M'$  are the nuclear masses for isotopes  $A$  and  $A'$ , respectively. The electronic factor  $K_{MS}$  is defined by,

$$\frac{K_{MS}}{M} \equiv \langle \Psi(PJM) | H_{MS} | \Psi(PJM) \rangle, \quad (13)$$

where

$$H_{MS} = \frac{1}{2M} \sum_{i,j} p_i \cdot p_j. \quad (14)$$

The mass shift operator (Eq. (14)) can be split into two parts, namely, the one-body and the two-body mass shift operators

$$H_{NMS} = \frac{1}{2M} \sum_i p_i^2 \quad (15)$$

**Table A**

Energy in ( $\text{cm}^{-1}$ ) relativistic normal mass shift  $\Delta K_{NMS}$ , specific mass shift  $\Delta K_{SMS}$  parameters (in GHz u) and field shift parameters  $\Delta FS$  (in GHz/fm $^2$ ) of the  $1s^2 \ ^1S_0 - 1s2p \ ^3P_0^o$  transitions of some He-like ions with MCDHF/RCI method in Breit + QED model. The label ( $n = y$ ) specifies the orbital active set.

Z	Model	$1s^2 \ ^1S_0 - 1s2p \ ^3P_0^o$				$1s^2 \ ^1S_0 - 1s2p \ ^3P_2^o$			
		Energy	$\Delta K_{NMS}$	$\Delta K_{SMS}$	$\Delta FS$	Energy	$\Delta K_{NMS}$	$\Delta K_{SMS}$	$\Delta FS$
7	MR ( $n = 2$ )	3 417 945	-5.628E+04	-1.017E+04	-3.490E+00	3 418 242	-5.629E+04	-1.019E+04	-3.499E+00
7	AS3 ( $n = 3$ )	3 436 421	-5.654E+04	-1.319E+04	-3.170E+00	3 436 718	-5.653E+04	-1.321E+04	-3.170E+00
7	AS4 ( $n = 4$ )	3 437 315	-5.641E+04	-1.322E+04	-3.162E+00	3 437 613	-5.640E+04	-1.323E+04	-3.162E+00
7	AS5 ( $n = 5$ )	3 437 705	-5.649E+04	-1.322E+04	-3.169E+00	3 438 003	-5.648E+04	-1.324E+04	-3.169E+00
33	MR ( $n = 2$ )	87 776 330	-1.450E+06	-2.803E+05	-2.598E+03	87 806 050	-1.457E+06	-2.831E+05	-2.601E+03
33	AS3 ( $n = 3$ )	87 798 194	-1.416E+06	-2.957E+05	-2.542E+03	88 173 301	-1.421E+06	-3.000E+05	-2.545E+03
33	AS4 ( $n = 4$ )	87 799 539	-1.415E+06	-2.956E+05	-2.539E+03	88 174 694	-1.420E+06	-3.000E+05	-2.542E+03
33	AS5 ( $n = 5$ )	87 800 283	-1.415E+06	-2.957E+05	-2.540E+03	88 175 439	-1.420E+06	-3.001E+05	-2.543E+03
83	MR ( $n = 2$ )	614 504 340	-8.252E+06	-1.169E+06	-4.902E+05	635 522 403	-8.579E+06	-1.573E+06	-4.977E+05
83	AS3 ( $n = 3$ )	614 553 981	-8.164E+06	-1.187E+06	-4.840E+05	635 577 612	-8.459E+06	-1.608E+06	-4.907E+05
83	AS4 ( $n = 4$ )	614 560 410	-8.163E+06	-1.176E+06	-4.833E+05	635 585 335	-8.453E+06	-1.599E+06	-4.901E+05
83	AS5 ( $n = 5$ )	614 569 084	-8.166E+06	-1.164E+06	-4.836E+05	635 594 009	-8.456E+06	-1.586E+06	-4.904E+05

**Table B**

Energy in ( $\text{cm}^{-1}$ ) relativistic normal mass shift  $\Delta K_{NMS}$ , specific mass shift  $\Delta K_{SMS}$  parameters (in GHz u) and field shift parameters  $\Delta FS$  (in GHz/fm $^2$ ) of the  $1s^2 \ ^1S_0 - 1s2p \ ^3\ ^1P_1^o$  transitions of some He-like ions with MCDHF/RCI method in Breit + QED model. The label ( $n = y$ ) specifies the orbital active set.

Z	Model	$1s^2 \ ^1S_0 - 1s2p \ ^3P_1^o$				$1s^2 \ ^1S_0 - 1s2p \ ^1P_1^o$			
		Energy	$\Delta K_{NMS}$	$\Delta K_{SMS}$	$\Delta FS$	Energy	$\Delta K_{NMS}$	$\Delta K_{SMS}$	$\Delta FS$
7	MR ( $n = 2$ )	3 417 953	-5.629E+04	-9.969E+03	-3.490E+00	3 455 883	-5.689E+04	9.767E+03	-3.490E+00
7	AS3 ( $n = 3$ )	3 436 428	-5.653E+04	-1.320E+04	-3.170E+00	3 472 308	-5.673E+04	6.900E+03	-3.120E+00
7	AS4 ( $n = 4$ )	3 437 323	-5.640E+04	-1.322E+04	-3.162E+00	3 473 111	-5.692E+04	6.744E+03	-3.116E+00
7	AS5 ( $n = 5$ )	3 437 713	-5.648E+04	-1.323E+04	-3.169E+00	3 473 501	-5.699E+04	6.739E+03	-3.124E+00
33	MR ( $n = 2$ )	87 798 724	-1.451E+06	-1.858E+05	-2.598E+03	88 330 229	-1.457E+06	1.867E+05	-2.601E+03
33	AS3 ( $n = 3$ )	87 820 201	-1.415E+06	-2.017E+05	-2.540E+03	88 349 801	-1.422E+06	1.681E+05	-2.538E+03
33	AS4 ( $n = 4$ )	87 821 556	-1.414E+06	-2.017E+05	-2.538E+03	88 351 084	-1.422E+06	1.675E+05	-2.535E+03
33	AS5 ( $n = 5$ )	87 822 301	-1.414E+06	-2.018E+05	-2.538E+03	88 351 828	-1.423E+06	1.674E+05	-2.536E+03
83	MR ( $n = 2$ )	613 951 634	-8.252E+06	-4.029E+05	-4.902E+05	635 984 641	-8.579E+06	5.377E+05	-4.977E+05
83	AS3 ( $n = 3$ )	614 005 077	-8.138E+06	-4.315E+05	-4.833E+05	636 036 613	-8.467E+06	5.049E+05	-4.902E+05
83	AS4 ( $n = 4$ )	614 012 626	-8.134E+06	-4.220E+05	-4.827E+05	636 044 215	-8.463E+06	5.139E+05	-4.897E+05
83	AS5 ( $n = 5$ )	614 021 300	-8.137E+06	-4.098E+05	-4.830E+05	636 052 889	-8.466E+06	5.261E+05	-4.900E+05

**Table C**

Mass shift  $MS$ , field shift  $FS$  and total isotope shift  $IS$  parameters (in GHz) of the  $1s^2 \ ^1S_0 - 1s2p \ ^3P_0^o$  transitions of some He-like ions with MCDHF/RCI method in Breit + QED model. The label ( $n = y$ ) specifies the orbital active set.

Z	Model	$1s^2 \ ^1S_0 - 1s2p \ ^3P_0^o$			$1s^2 \ ^1S_0 - 1s2p \ ^3P_2^o$		
		$MS$	$FS$	$IS$	$MS$	$FS$	$IS$
7	MR ( $n = 2$ )	3.280E+02	-8.435E-01	3.272E+02	3.281E+02	-8.435E-01	3.273E+02
7	AS3 ( $n = 3$ )	3.320E+02	-7.644E-01	3.313E+02	3.321E+02	-7.644E-01	3.313E+02
7	AS4 ( $n = 4$ )	3.316E+02	-7.622E-01	3.308E+02	3.316E+02	-7.622E-01	3.308E+02
7	AS5 ( $n = 5$ )	3.108E+02	-7.641E-01	3.101E+02	3.109E+02	-7.641E-01	3.101E+02
33	MR ( $n = 2$ )	3.113E+02	-3.295E+02	-1.826E+01	3.130E+02	-3.300E-01	-1.702E+01
33	AS3 ( $n = 3$ )	3.085E+02	-3.225E+02	-1.404E+01	3.101E+02	-3.229E+02	-1.275E+01
33	AS4 ( $n = 4$ )	3.083E+02	-3.221E+02	-1.385E+01	3.099E+02	-3.225E+02	-1.257E+01
33	AS5 ( $n = 5$ )	3.077E+02	-3.222E+02	-1.447E+01	3.094E+02	-3.226E+02	-1.319E+01
83	MR ( $n = 2$ )	2.166E+02	-3.970E+04	-3.948E+04	2.334E+02	-4.031E+04	-4.007E+04
83	AS3 ( $n = 3$ )	2.151E+02	-3.919E+04	-3.898E+04	2.316E+02	-3.974E+04	-3.951E+04
83	AS4 ( $n = 4$ )	2.148E+02	-3.914E+04	-3.892E+04	2.312E+02	-3.969E+04	-3.946E+04
83	AS5 ( $n = 5$ )	2.145E+02	-3.917E+04	-3.895E+04	2.309E+02	-3.972E+04	-3.949E+04

$$H_{SMS} = \frac{1}{2M} \sum_{i \neq j} \mathbf{p}_i \cdot \mathbf{p}_j, \quad (16)$$

which are also called the normal mass shift (NMS) and the specific mass shift (named also mass polarization (SMS) operator), respectively.

### 3. Generation of configuration expansions MCDHF/RCI

As a starting point, MCDHF/RCI calculations in the *EOL* scheme were performed for each group of atomic states. Using configuration expansions including all lower states of the same  $J$  symmetry and parity, and a Dirac–Coulomb version was used. For the optimization of the orbitals, we include Breit corrections in a final configuration interaction calculation [14]. To build a CSF expansion, the restrictive active space methods were also used. The idea of the active space

methods is to consider only electrons from the active space and to excite them from the occupied orbitals to unoccupied ones. The orbital was increased systematically in order to monitor the convergence of the calculation. Since the orbitals with the same principal quantum number  $n$  often have similar energies, the active set is usually enlarged in steps of orbital layers. It is convenient to refer to the  $\{1s, \dots, 3l \mid l = 0 - 2\}$  set of orbitals as the  $n = 3$  orbital layer,  $\{1s, \dots, 4l \mid l = 0 - 3\}$  as the  $n = 4$  layer, etc. The active sets are extended to  $n = 5$ . In all steps, only new orbitals are optimized. For example, in the first calculation for the multireference MR ( $n = 2$ ) all orbitals are optimized. In the next step, the orbitals of MR ( $n = 2$ ) are frozen and only the new orbitals  $\{3l \mid l = 0 - 2\}$  from the active set (AS<sub>3</sub>) are optimized. Only the outermost  $nl$ -orbitals are optimized while the inside ones are fixed.

**Table D**

Mass shift  $MS$ , field shift  $FS$  and total isotope shift  $IS$  parameters (in GHz) of the  $1s^2 \ ^1S_0 - 1s\ 2p \ ^3P_1^o$  transitions of some He-like ions with MCDHF/RCI method in Breit + QED model. The label ( $n = y$ ) specifies the orbital active set.

Z	Model	$1s^2 \ ^1S_0 - 1s\ 2p \ ^3P_1^o$			$1s^2 \ ^1S_0 - 1s\ 2p \ ^1P_1^o$		
		$MS$	$FS$	$IS$	$MS$	$FS$	$IS$
7	MR ( $n = 2$ )	3.281E+02	-8.435E-01	3.272E+02	2.372E+02	-8.435E-01	2.364E+02
7	AS3 ( $n = 3$ )	3.320E+02	-7.643E-01	3.313E+02	2.373E+02	-7.522E-01	2.365E+02
7	AS4 ( $n = 4$ )	3.316E+02	-7.622E-01	3.308E+02	2.389E+02	-7.513E-01	2.381E+02
7	AS5 ( $n = 5$ )	3.108E+02	-7.641E-01	3.101E+02	2.241E+02	-7.532E-01	2.233E+02
33	MR ( $n = 2$ )	2.943E+02	-3.296E+01	-3.522E+01	2.284E+02	-3.300E+02	-1.015E+01
33	AS3 ( $n = 3$ )	2.914E+02	-3.223E+02	-3.089E+01	2.260E+02	-3.219E+02	-9.586E+01
33	AS4 ( $n = 4$ )	2.912E+02	-3.219E+02	-3.068E+01	2.261E+02	-3.216E+02	-9.547E+01
33	AS5 ( $n = 5$ )	2.907E+02	-3.220E+02	-3.127E+01	2.257E+02	-3.217E+02	-9.593E+01
83	MR ( $n = 2$ )	1.989E+02	-3.970E+04	-3.950E+04	1.848E+02	-4.031E+04	-4.012E+04
83	AS3 ( $n = 3$ )	1.971E+02	-3.914E+04	-3.894E+04	1.831E+02	-3.970E+04	-3.952E+04
83	AS4 ( $n = 4$ )	1.968E+02	-3.909E+04	-3.889E+04	1.828E+02	-3.966E+04	-3.948E+04
83	AS5 ( $n = 5$ )	1.965E+02	-3.912E+04	-3.892E+04	1.825E+02	-3.969E+04	-3.950E+04

## 4. Results and discussion

### 4.1. Correlation effects on isotope shifts

Being interested in the isoelectronic helium sequence and the importance of correlation effects for some ions we choose ( $N^{6+}$ ,  $As^{32+}$  and  $Bi^{82+}$ ). For that, we present in **Tables A** and **B** energy in ( $cm^{-1}$ ), relativistic normal mass shift  $\Delta K_{NMS}$ , specific mass shift  $\Delta K_{SMS}$  parameters (in GHz u) and field shift  $\Delta FS$  (in GHz/fm $^2$ ) factors of the  $1s^2 \ ^1S_0 - 1s\ 2p \ ^3P_0^o$  and the  $1s^2 \ ^1S_0 - 1s\ 2p \ ^3P_1^o$  transitions as function of the increasing orbital active set. As can be seen from these tables, the relativistic normal- and specific-mass shifts, energy and field shift factor in these transitions are sensitive to correlation. A complete convergence of these physical quantities is achieved between AS4 and AS5 active set models. We find that average relative variations between the two consecutive active set models within 0.01%, 0.1%, 0.1% and 0.2% respectively for the energy, normal mass shift, specific mass shift and field shift. In **Tables C** and **D**, we present Mass shift  $MS$ , Field shift  $FS$  and total isotope shift  $IS$  parameters (in GHz) of the  $1s^2 \ ^1S_0 - 1s\ 2p \ ^3P_0^o$  and  $1s^2 \ ^1S_0 - 1s\ 2p \ ^3P_1^o$  transitions as function of the increasing orbital active set. In the layer by layer calculations, we noticed that the convergence is assured.

To check the reliability of our computational method, the mass- and field shifts parameters of the  $1s^2 \ ^1S_0 - 1s\ 2p \ ^1P_1^o$  and  $1s^2 \ ^1S_0 - 1s\ 2p \ ^3P_{0,1,2}^o$  transitions in He-like ions are presented in **Tables E** and **F** and compared against results of Zubova et al. [11] obtained by using the Dirac-Fock-Sturm method. Our results are in reasonable agreement with Ref. [11]. The difference is within around 3% and 17% for the MS and FS parameters for these transitions, respectively. In fact, in **Table E** we present  $1s^2 \ ^1S_0 - 1s\ 2p \ ^3P_0^o$  transitions and in **Table F** we list  $1s^2 \ ^1S_0 - 1s\ 2p \ ^1P_1^o$  and  $1s^2 \ ^1S_0 - 1s\ 2p \ ^3P_1^o$ . We notices that for both tables the  $\Delta MS$  variation is around 2% and for heavy ions such as  $Hg^{78+}$  difference reaches 8%. On the other hand,  $\Delta FS$  variation is 4% for  $Mg^{10+}$ ,  $Ca^{18+}$ ,  $Zn^{28+}$ ,  $Zr^{38+}$  and  $Sn^{48+}$ . These differences exceed 15% for  $Nd^{58+}$ ,  $Yb^{68+}$  and  $Hg^{78+}$ .

### 4.2. Behavior of NMS, SMS and FS

**Fig. 1** shows the variation between the normal mass shifts and specific mass shifts as function of  $Z$ . For  $1s^2 \ ^1S_0 - 1s\ 2p \ ^3P_0^o$  transitions, it is shown that these two contribution terms evolve in the same direction. This means both NMS and SMS shifts decrease with  $Z$  in the negative region. In the  $1s^2 \ ^1S_0 - 1s\ 2p \ ^1P_1^o$  E1 type transition case, NMS and SMS contributions vary in opposite directions. As function of  $Z$ , the SMS shift contribution increases starting from zero however the NMS shift contribution decreases starting from zero.

For the high-Z region ( $20 \leq Z$ ), we have a minimum value for the NMS parameters that reach  $-8 \times 10^6$  GHz u. For these transitions, the

**Table E**

$\Delta FS$  parameters (in GHz/fm $^2$ ) and Mass shift  $\Delta MS$  in terms of the K-factor (in 1000 GHz a.m.u.) of the  $1s^2 \ ^1S_0 - 1s\ 2p \ ^3P_0^o$  transitions of He-like ions compared to  $\Delta FS$  and  $\Delta MS$  obtained with Zubova et al. [11].

Z	$1s^2 \ ^1S_0 - 1s\ 2p \ ^3P_0^o$		$1s^2 \ ^1S_0 - 1s\ 2p \ ^3P_2^o$	
	$\Delta FS$	$\Delta FS$ [11]	$\Delta FS$	$\Delta FS$ [11]
$Mg^{10+}$	-3.080E+01	-3.067E+01	-3.080E+01	-3.068E+01
$Ca^{18+}$	-2.708E+02	-2.685E+02	-2.709E+02	-2.686E+02
$Zn^{28+}$	-1.635E+03	-1.610E+03	-1.637E+03	-1.612E+03
$Zr^{38+}$	-6.399E+03	-6.253E+03	-6.410E+03	-6.264E+03
$Sn^{48+}$	-2.015E+04	-1.948E+04	-2.022E+04	-1.954E+03
$Nd^{58+}$	-5.634E+04	-5.377E+04	-5.663E+04	-5.406E+04
$Yb^{68+}$	-1.467E+05	-1.371E+05	-1.479E+05	-1.382E+05
$Hg^{78+}$	-3.683E+05	-3.400E+05	-3.729E+05	-3.444E+05

Z	$1s^2 \ ^1S_0 - 1s\ 2p \ ^3P_0^o$		$1s^2 \ ^1S_0 - 1s\ 2p \ ^3P_2^o$	
	$\Delta MS$	$\Delta MS$ [11]	$\Delta MS$	$\Delta MS$ [11]
$Mg^{10+}$	-217	-217.74	-217	-217.85
$Ca^{18+}$	-622	-626.50	-623	-627.50
$Zn^{28+}$	-1410	-1447	-1420	-1453
$Zr^{38+}$	-2510	-2650	-2530	-2670
$Sn^{48+}$	-3890	-4315	-3950	-4368
$Nd^{58+}$	-5510	-6601	-5640	-6723
$Yb^{68+}$	-7250	-9802	-7540	-12077
$Hg^{78+}$	-8910	-14500	-9490	-15020

**Table F**

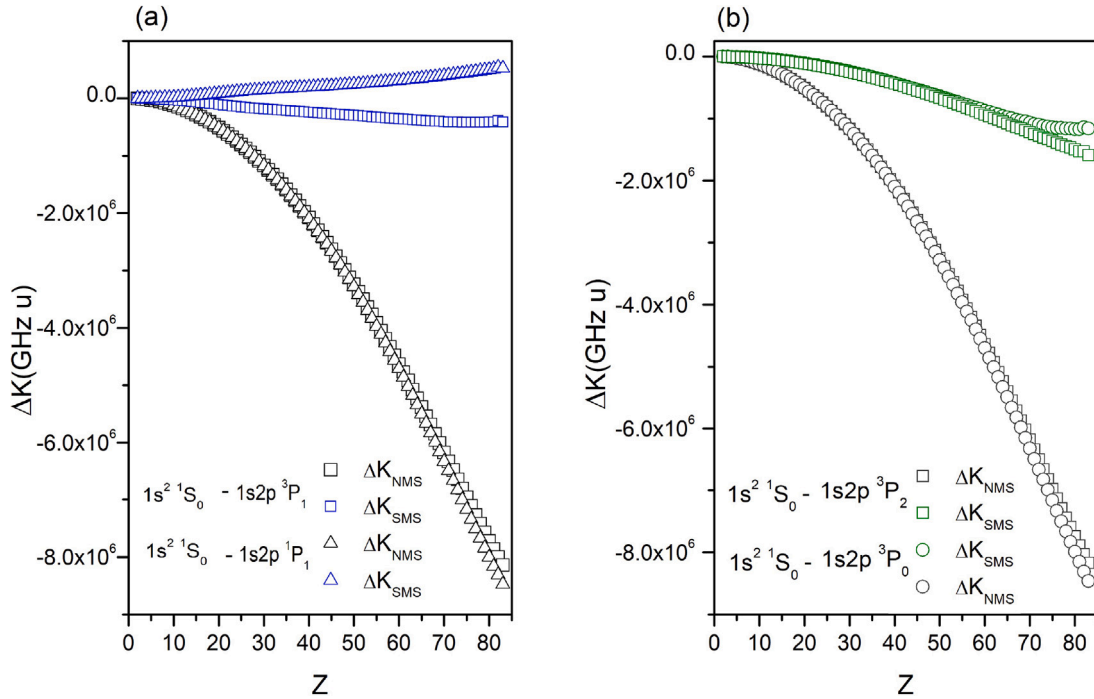
$\Delta FS$  parameters (in GHz/fm $^2$ ) and Mass shift  $\Delta MS$  in terms of the K-factor (in 1000 GHz a.m.u.) of the  $1s^2 \ ^1S_0 - 1s\ 2p \ ^3P_1^o$  and  $1s^2 \ ^1S_0 - 1s\ 2p \ ^1P_1^o$  transitions of He-like ions compared to  $\Delta FS$  and  $\Delta MS$  obtained with Zubova et al. [11].

Z	$1s^2 \ ^1S_0 - 1s\ 2p \ ^3P_1^o$		$1s^2 \ ^1S_0 - 1s\ 2p \ ^1P_1^o$	
	$\Delta FS$	$\Delta FS$ [11]	$\Delta FS$	$\Delta FS$ [11]
$Mg^{10+}$	-3.079E+01	-3.041E+01	-3.053E+01	-3.067E+01
$Ca^{18+}$	-2.708E+02	-2.671E+02	-2.695E+02	-2.684E+02
$Zn^{28+}$	-1.634E+03	-1.606E+03	-1.632E+03	-1.609E+03
$Zr^{38+}$	-6.394E+03	-6.251E+03	-6.397E+03	-6.248E+03
$Sn^{48+}$	-2.013E+04	-1.951E+04	-2.018E+04	-1.946E+04
$Nd^{58+}$	-5.628E+04	-5.399E+04	-5.656E+04	-5.372E+04
$Yb^{68+}$	-1.466E+05	-1.381E+05	-1.478E+05	-1.369E+05
$Hg^{78+}$	-3.679E+05	-3.439E+05	-3.726E+05	-3.397E+05

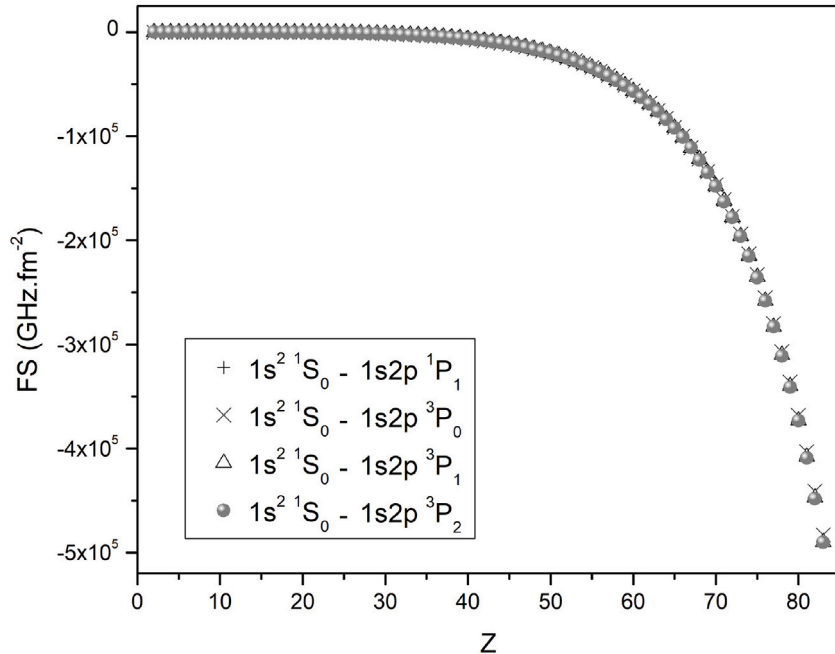
  

Z	$1s^2 \ ^1S_0 - 1s\ 2p \ ^3P_1^o$		$1s^2 \ ^1S_0 - 1s\ 2p \ ^1P_1^o$	
	$\Delta MS$	$\Delta MS$ [11]	$\Delta MS$	$\Delta MS$ [11]
$Mg^{10+}$	-217	-217.65	-151	-151.35
$Ca^{18+}$	-616	-621.1	-428	-433.5
$Zn^{28+}$	-1350	-1385	-1020	-1054
$Zr^{38+}$	-2320	-2458	-1900	-2037
$Sn^{48+}$	-3540	-3956	-3040	-3450
$Nd^{58+}$	-4980	-6053	-4400	-5462
$Yb^{68+}$	-6570	-9052	-5930	-8404
$Hg^{78+}$	-8130	-13540	-7500	-12930

SMS and NMS parameters both change monotonously with increasing  $Z$ , as shown in **Fig. 1**.



**Fig. 1.** The  $\Delta K_{NMS}$  and  $\Delta K_{SMS}$  parameters in (GHz  $u$ ) of the  $1s^2 \ ^1S_0 - 1s2p \ ^1P_1^o$  and  $1s^2 \ ^1S_0 - 1s2p \ ^3P_{0,1,2}^o$  transitions in He-like ions as a function of the nuclear charge number  $Z$ .



**Fig. 2.** Field shift (FS) parameters in GHz  $fm^{-2}$  of  $1s^2 \ ^1S_0 - 1s2p \ ^1P_1^o$  and  $1s^2 \ ^1S_0 - 1s2p \ ^3P_{0,1,2}^o$  transitions in He-like ions as a function of the nuclear charge number  $Z$  with  $2 \leq Z \leq 83$ .

**Fig. 2** shows the behavior of the field shifts FS in unit of GHz  $fm^{-2}$  as a function of  $Z$  ( $2 \leq Z \leq 83$ ) of the  $1s^2 \ ^1S_0 - 1s2p \ ^1P_1^o$  and  $1s^2 \ ^1S_0 - 1s2p \ ^3P_{0,1,2}^o$  transitions. As can be noticed, in the region of  $2 \leq Z \leq 40$  the field shift is quite constant. Then, for high nuclear charge number  $Z$  the FS drastically decreased around  $-4.8 \times 10^5$  GHz  $fm^{-2}$ .

#### 4.3. Balance between mass- and field-shifts

Using the MCDHF/RCI results from Tables 1 and 2, we illustrate in Figs. 3 and 4 the absolute value of  $|\delta\nu_{MS}|$  and  $|\delta\nu_{FS}|$  for  $1s^2 \ ^1S_0$

$- 1s2p \ ^1P_1^o$  and  $1s^2 \ ^1S_0 - 1s2p \ ^3P_{0,1,2}^o$  transitions in He-like ions with  $2 \leq Z \leq 83$  for the isotope pair (A,A + 1). The balance between the mass shifts (MS) and the field shifts (FS) can be noticed from these four figures. As can be seen, in the region of  $2 \leq Z \leq 33$  the mass shift is quite larger than the field shift for the transitions concerned and of the same order of magnitude with an average of 300 GHz. So that, for a relevant analysis of isotope shifts (IS) both of the mass shift and field shift must be taken into account. In the region of  $34 \leq Z$ , the mass shift is inferior to the field shift for the transitions mentioned above. In fact, the mass shifts can be considered as constant, and the field shifts

**Table 1**

NMS, SMS parameters (in GHz u) and FS parameters (in GHz/fm<sup>2</sup>) of the  $1s^2 \ ^1S_0 - 1s\ 2p\ ^3P_{0,2}^o$  transitions of He-like ions from  $Z = 2$  to  $Z = 83$  with MCDHF/RCI method in Breit + QED model.

Z	$1s^2 \ ^1S_0 - 1s\ 2p\ ^3P_0^o$			$1s^2 \ ^1S_0 - 1s\ 2p\ ^3P_2^o$		
	$\Delta K_{NMS}$	$\Delta K_{SMS}$	$\Delta FS$	$\Delta K_{NMS}$	$\Delta K_{SMS}$	$\Delta FS$
He	-2.771E+03	-8.142E+02	-1.086E-02	-2.771E+03	-8.143E+02	-1.086E-02
Li <sup>1+</sup>	-8.118E+03	-2.153E+03	-7.752E-02	-8.117E+03	-2.154E+03	-7.752E-02
Be <sup>2+</sup>	-1.616E+04	-4.074E+03	-2.833E-01	-1.616E+04	-4.076E+03	-2.833E-01
B <sup>3+</sup>	-2.690E+04	-6.562E+03	-7.511E-01	-2.690E+04	-6.567E+03	-7.511E-01
C <sup>4+</sup>	-4.035E+04	-9.614E+03	-1.644E+00	-4.034E+04	-9.623E+03	-1.644E+00
N <sup>5+</sup>	-5.649E+04	-1.323E+04	-3.170E+00	-5.648E+04	-1.324E+04	-3.170E+00
O <sup>6+</sup>	-7.533E+04	-1.740E+04	-5.578E+00	-7.533E+04	-1.743E+04	-5.578E+00
F <sup>7+</sup>	-9.688E+04	-2.213E+04	-9.168E+00	-9.687E+04	-2.217E+04	-9.168E+00
Ne <sup>8+</sup>	-1.211E+05	-2.742E+04	-2.134E+01	-1.211E+05	-2.748E+04	-2.134E+01
Na <sup>9+</sup>	-1.480E+05	-3.327E+04	-1.429E+01	-1.480E+05	-3.334E+04	-1.429E+01
Mg <sup>10+</sup>	-1.777E+05	-3.966E+04	-3.080E+01	-1.777E+05	-3.977E+04	-3.080E+01
Al <sup>11+</sup>	-2.100E+05	-4.661E+04	-4.316E+01	-2.100E+05	-4.675E+04	-4.316E+01
Si <sup>12+</sup>	-2.450E+05	-5.411E+04	-5.904E+01	-2.450E+05	-5.428E+04	-5.904E+01
P <sup>13+</sup>	-2.827E+05	-6.215E+04	-7.907E+01	-2.828E+05	-6.238E+04	-7.908E+01
S <sup>14+</sup>	-3.231E+05	-7.073E+04	-1.040E+02	-3.232E+05	-7.102E+04	-1.040E+02
Cl <sup>15+</sup>	-3.661E+05	-7.986E+04	-1.347E+02	-3.663E+05	-8.022E+04	-1.347E+02
Ar <sup>16+</sup>	-4.118E+05	-8.952E+04	-1.719E+02	-4.121E+05	-8.996E+04	-1.720E+02
K <sup>17+</sup>	-4.602E+05	-9.972E+04	-2.170E+02	-4.605E+05	-1.003E+05	-2.170E+02
Ca <sup>18+</sup>	-5.113E+05	-1.104E+05	-2.708E+02	-5.117E+05	-1.111E+05	-2.709E+02
Sc <sup>19+</sup>	-5.650E+05	-1.217E+05	-3.344E+02	-5.655E+05	-1.225E+05	-3.345E+02
Ti <sup>20+</sup>	-6.214E+05	-1.335E+05	-4.095E+02	-6.221E+05	-1.344E+05	-4.096E+02
V <sup>21+</sup>	-6.805E+05	-1.458E+05	-4.974E+02	-6.813E+05	-1.468E+05	-4.976E+02
Cr <sup>22+</sup>	-7.422E+05	-1.586E+05	-6.000E+02	-7.432E+05	-1.598E+05	-6.003E+02
Mn <sup>23+</sup>	-8.065E+05	-1.719E+05	-7.188E+02	-8.077E+05	-1.733E+05	-7.191E+02
Fe <sup>24+</sup>	-8.735E+05	-1.857E+05	-8.562E+02	-8.750E+05	-1.874E+05	-8.567E+02
Co <sup>25+</sup>	-9.431E+05	-2.000E+05	-1.014E+03	-9.449E+05	-2.020E+05	-1.014E+03
Ni <sup>26+</sup>	-1.015E+06	-2.148E+05	-1.195E+03	-1.017E+06	-2.170E+05	-1.196E+03
Cu <sup>27+</sup>	-1.090E+06	-2.300E+05	-1.400E+03	-1.093E+06	-2.327E+05	-1.401E+03
Zn <sup>28+</sup>	-1.168E+06	-2.458E+05	-1.635E+03	-1.171E+06	-2.488E+05	-1.637E+03
Ga <sup>29+</sup>	-1.248E+06	-2.620E+05	-1.900E+03	-1.251E+06	-2.654E+05	-1.902E+03
Ge <sup>30+</sup>	-1.330E+06	-2.786E+05	-2.201E+03	-1.334E+06	-2.825E+05	-2.203E+03
As <sup>31+</sup>	-1.416E+06	-2.958E+05	-2.540E+03	-1.420E+06	-3.002E+05	-2.543E+03
Se <sup>32+</sup>	-1.504E+06	-3.133E+05	-2.921E+03	-1.509E+06	-3.183E+05	-2.925E+03
Br <sup>33+</sup>	-1.594E+06	-3.313E+05	-3.352E+03	-1.600E+06	-3.369E+05	-3.356E+03
Kr <sup>34+</sup>	-1.687E+06	-3.497E+05	-3.832E+03	-1.694E+06	-3.560E+05	-3.837E+03
Rb <sup>35+</sup>	-1.783E+06	-3.685E+05	-4.373E+03	-1.790E+06	-3.755E+05	-4.379E+03
Sr <sup>36+</sup>	-1.881E+06	-3.877E+05	-4.974E+03	-1.889E+06	-3.956E+05	-4.982E+03
Y <sup>37+</sup>	-1.981E+06	-4.073E+05	-5.649E+03	-1.991E+06	-4.161E+05	-5.658E+03
Zr <sup>38+</sup>	-2.084E+06	-4.272E+05	-6.399E+03	-2.095E+06	-4.370E+05	-6.410E+03
Nb <sup>39+</sup>	-2.190E+06	-4.475E+05	-7.234E+03	-2.202E+06	-4.584E+05	-7.247E+03
Mo <sup>40+</sup>	-2.298E+06	-4.682E+05	-8.158E+03	-2.312E+06	-4.803E+05	-8.175E+03
Tc <sup>41+</sup>	-2.408E+06	-4.891E+05	-9.187E+03	-2.424E+06	-5.025E+05	-9.207E+03
Ru <sup>42+</sup>	-2.521E+06	-5.103E+05	-1.032E+04	-2.538E+06	-5.251E+05	-1.035E+04
Rh <sup>43+</sup>	-2.637E+06	-5.319E+05	-1.159E+04	-2.656E+06	-5.483E+05	-1.162E+04
Pd <sup>44+</sup>	-2.754E+06	-5.537E+05	-1.298E+04	-2.775E+06	-5.719E+05	-1.301E+04
Ag <sup>45+</sup>	-2.875E+06	-5.758E+05	-1.453E+04	-2.897E+06	-5.958E+05	-1.456E+04
Cd <sup>46+</sup>	-2.997E+06	-5.981E+05	-1.622E+04	-3.022E+06	-6.201E+05	-1.627E+04
In <sup>47+</sup>	-3.122E+06	-6.205E+05	-1.809E+04	-3.149E+06	-6.448E+05	-1.815E+04
Sn <sup>48+</sup>	-3.249E+06	-6.432E+05	-2.015E+04	-3.279E+06	-6.698E+05	-2.022E+04
Sb <sup>49+</sup>	-3.378E+06	-6.659E+05	-2.243E+04	-3.411E+06	-6.952E+05	-2.250E+04
Te <sup>50+</sup>	-3.509E+06	-6.888E+05	-2.490E+04	-3.545E+06	-7.209E+05	-2.499E+04
I <sup>51+</sup>	-3.643E+06	-7.118E+05	-2.769E+04	-3.682E+06	-7.470E+05	-2.780E+04
Xe <sup>52+</sup>	-3.779E+06	-7.348E+05	-3.071E+04	-3.821E+06	-7.733E+05	-3.083E+04
Cs <sup>53+</sup>	-3.917E+06	-7.578E+05	-3.405E+04	-3.963E+06	-8.000E+05	-3.419E+04
Ba <sup>54+</sup>	-4.057E+06	-7.808E+05	-3.769E+04	-4.107E+06	-8.269E+05	-3.785E+04
La <sup>55+</sup>	-4.198E+06	-8.038E+05	-4.172E+04	-4.253E+06	-8.541E+05	-4.190E+04
Ce <sup>56+</sup>	-4.342E+06	-8.266E+05	-4.616E+04	-4.401E+06	-8.815E+05	-4.637E+04
Pr <sup>57+</sup>	-4.488E+06	-8.492E+05	-5.103E+04	-4.551E+06	-9.092E+05	-5.128E+04
Nd <sup>58+</sup>	-4.635E+06	-8.717E+05	-5.634E+04	-4.703E+06	-9.370E+05	-5.663E+04
Pm <sup>59+</sup>	-4.785E+06	-8.939E+05	-6.220E+04	-4.858E+06	-9.651E+05	-6.254E+04
Sm <sup>60+</sup>	-4.935E+06	-9.158E+05	-6.851E+04	-5.014E+06	-9.933E+05	-6.890E+04
Eu <sup>61+</sup>	-5.087E+06	-9.373E+05	-7.552E+04	-5.172E+06	-1.022E+06	-7.597E+04
Gd <sup>62+</sup>	-5.240E+06	-9.584E+05	-8.308E+04	-5.331E+06	-1.050E+06	-8.360E+04
Tb <sup>63+</sup>	-5.395E+06	-9.789E+05	-9.148E+04	-5.493E+06	-1.079E+06	-9.207E+04
Dy <sup>64+</sup>	-5.551E+06	-9.989E+05	-1.006E+05	-5.655E+06	-1.107E+06	-1.013E+05
Ho <sup>65+</sup>	-5.708E+06	-1.018E+06	-1.106E+05	-5.819E+06	-1.136E+06	-1.114E+05
Er <sup>66+</sup>	-5.866E+06	-1.037E+06	-1.216E+05	-5.985E+06	-1.165E+06	-1.226E+05
Tm <sup>67+</sup>	-6.024E+06	-1.055E+06	-1.337E+05	-6.152E+06	-1.193E+06	-1.347E+05
Yb <sup>68+</sup>	-6.183E+06	-1.071E+06	-1.467E+05	-6.319E+06	-1.222E+06	-1.479E+05
Lu <sup>69+</sup>	-6.343E+06	-1.087E+06	-1.612E+05	-6.487E+06	-1.250E+06	-1.625E+05
Hf <sup>70+</sup>	-6.502E+06	-1.102E+06	-1.768E+05	-6.656E+06	-1.279E+06	-1.784E+05

(continued on next page)

**Table 1** (continued).

Ta <sup>71+</sup>	-6.661E+06	-1.115E+06	-1.940E+05	-6.824E+06	-1.307E+06	-1.958E+05
W <sup>72+</sup>	-6.819E+06	-1.127E+06	-2.127E+05	-6.993E+06	-1.335E+06	-2.148E+05
Re <sup>73+</sup>	-6.978E+06	-1.138E+06	-2.334E+05	-7.162E+06	-1.362E+06	-2.357E+05
Os <sup>74+</sup>	-7.134E+06	-1.146E+06	-2.556E+05	-7.330E+06	-1.390E+06	-2.583E+05
Ir <sup>75+</sup>	-7.290E+06	-1.154E+06	-2.803E+05	-7.498E+06	-1.418E+06	-2.833E+05
Pt <sup>76+</sup>	-7.443E+06	-1.160E+06	-3.071E+05	-7.663E+06	-1.445E+06	-3.106E+05
Au <sup>77+</sup>	-7.595E+06	-1.164E+06	-3.365E+05	-7.828E+06	-1.472E+06	-3.406E+05
Hg <sup>78+</sup>	-7.743E+06	-1.166E+06	-3.683E+05	-7.989E+06	-1.500E+06	-3.729E+05
Tl <sup>79+</sup>	-7.888E+06	-1.166E+06	-4.033E+05	-8.149E+06	-1.527E+06	-4.085E+05
Pb <sup>80+</sup>	-8.030E+06	-1.142E+06	-4.416E+05	-8.305E+06	-1.533E+06	-4.476E+05
Bi <sup>81+</sup>	-8.166E+06	-1.164E+06	-4.836E+05	-8.457E+06	-1.587E+06	-4.905E+05

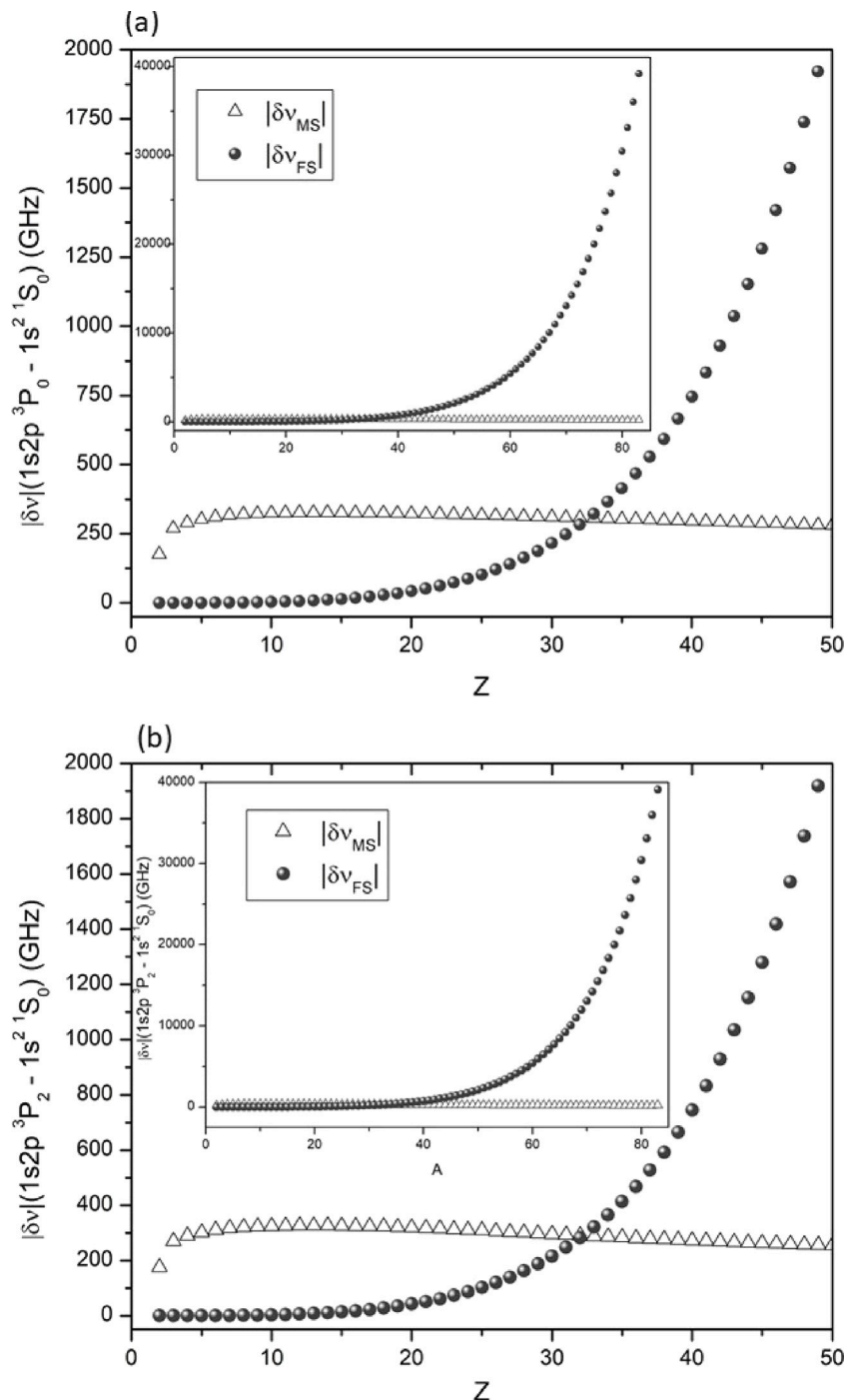


**Fig. 3.** Absolute value of the mass shifts  $|\delta v_{MS}|$  and field shifts  $|\delta v_{FS}|$  as functions of the nuclear charge  $2 \leq Z \leq 83$  (in GHz). Results are shown for  $1s^2 \ ^1S_0 - 1s \ 2p \ ^3P_0$  transitions calculated for the isotope pair (A, A + 1).

**Table 2**

NMS, SMS parameters (in GHz u) and FS parameters (in GHz/fm<sup>2</sup>) of the  $1s^2 \ ^1S_0 - 1s\ 2p\ (^3P_1^o, ^1P_1^o)$  transitions of He-like ions from  $Z = 2$  to  $Z = 83$  with MCDHF/RCI method in Breit + QED model.

Z	$1s^2 \ ^1S_0 - 1s\ 2p\ (^3P_1^o)$			$1s^2 \ ^1S_0 - 1s\ 2p\ (^1P_1^o)$		
	$\Delta K_{NMS}$	$\Delta K_{SMS}$	$\Delta FS$	$\Delta K_{NMS}$	$\Delta K_{SMS}$	$\Delta FS$
He	-2.771E+03	-8.143E+02	-1.086E-02	-2.802E+03	-4.192E+02	-1.056E-02
Li <sup>1+</sup>	-8.118E+03	-2.153E+03	-7.752E-02	-8.231E+03	-1.523E+02	-7.544E-02
Be <sup>2+</sup>	-1.616E+04	-4.075E+03	-2.833E-01	-1.637E+04	7.106E+02	-2.769E-01
B <sup>3+</sup>	-2.690E+04	-6.564E+03	-7.511E-01	-2.721E+04	2.153E+03	-7.368E-01
C <sup>4+</sup>	-4.034E+04	-9.618E+03	-1.644E+00	-4.075E+04	4.164E+03	-1.618E+00
N <sup>5+</sup>	-5.648E+04	-1.323E+04	-3.170E+00	-5.700E+04	6.740E+03	-3.125E+00
O <sup>6+</sup>	-7.533E+04	-1.741E+04	-5.578E+00	-7.594E+04	9.875E+03	-5.508E+00
F <sup>7+</sup>	-9.687E+04	-2.214E+04	-9.168E+00	-9.759E+04	1.357E+04	-9.064E+00
Ne <sup>8+</sup>	-1.211E+05	-2.742E+04	-2.134E+01	-1.219E+05	1.780E+04	-2.114E+01
Na <sup>9+</sup>	-1.480E+05	-3.325E+04	-1.429E+01	-1.490E+05	2.258E+04	-1.414E+01
Mg <sup>10+</sup>	-1.777E+05	-3.960E+04	-3.079E+01	-1.787E+05	2.789E+04	-3.053E+01
Al <sup>11+</sup>	-2.100E+05	-4.647E+04	-4.316E+01	-2.111E+05	3.370E+04	-4.281E+01
Si <sup>12+</sup>	-2.450E+05	-5.381E+04	-5.903E+01	-2.462E+05	4.000E+04	-5.860E+01
P <sup>13+</sup>	-2.826E+05	-6.161E+04	-7.906E+01	-2.840E+05	4.673E+04	-7.853E+01
S <sup>14+</sup>	-3.230E+05	-6.980E+04	-1.040E+02	-3.245E+05	5.387E+04	-1.034E+02
Cl <sup>15+</sup>	-3.661E+05	-7.834E+04	-1.347E+02	-3.677E+05	6.133E+04	-1.339E+02
Ar <sup>16+</sup>	-4.118E+05	-8.714E+04	-1.719E+02	-4.136E+05	6.906E+04	-1.710E+02
K <sup>17+</sup>	-4.602E+05	-9.612E+04	-2.170E+02	-4.622E+05	7.698E+04	-2.159E+02
Ca <sup>18+</sup>	-5.112E+05	-1.052E+05	-2.708E+02	-5.134E+05	8.497E+04	-2.695E+02
Sc <sup>19+</sup>	-5.649E+05	-1.143E+05	-3.344E+02	-5.673E+05	9.296E+04	-3.329E+02
Ti <sup>20+</sup>	-6.213E+05	-1.232E+05	-4.094E+02	-6.239E+05	1.008E+05	-4.077E+02
V <sup>21+</sup>	-6.803E+05	-1.320E+05	-4.973E+02	-6.832E+05	1.085E+05	-4.954E+02
Cr <sup>22+</sup>	-7.420E+05	-1.405E+05	-5.998E+02	-7.452E+05	1.160E+05	-5.978E+02
Mn <sup>23+</sup>	-8.063E+05	-1.487E+05	-7.185E+02	-8.098E+05	1.231E+05	-7.163E+02
Fe <sup>24+</sup>	-8.733E+05	-1.566E+05	-8.558E+02	-8.771E+05	1.298E+05	-8.534E+02
Co <sup>25+</sup>	-9.428E+05	-1.640E+05	-1.013E+03	-9.471E+05	1.362E+05	-1.011E+03
Ni <sup>26+</sup>	-1.015E+06	-1.711E+05	-1.194E+03	-1.020E+06	1.422E+05	-1.192E+03
Cu <sup>27+</sup>	-1.090E+06	-1.778E+05	-1.400E+03	-1.095E+06	1.478E+05	-1.397E+03
Zn <sup>28+</sup>	-1.167E+06	-1.842E+05	-1.634E+03	-1.173E+06	1.531E+05	-1.632E+03
Ga <sup>29+</sup>	-1.247E+06	-1.903E+05	-1.899E+03	-1.254E+06	1.581E+05	-1.896E+03
Ge <sup>30+</sup>	-1.330E+06	-1.962E+05	-2.199E+03	-1.337E+06	1.629E+05	-2.197E+03
As <sup>31+</sup>	-1.415E+06	-2.019E+05	-2.539E+03	-1.423E+06	1.675E+05	-2.536E+03
Se <sup>32+</sup>	-1.503E+06	-2.074E+05	-2.919E+03	-1.512E+06	1.719E+05	-2.917E+03
Br <sup>33+</sup>	-1.593E+06	-2.127E+05	-3.350E+03	-1.603E+06	1.762E+05	-3.348E+03
Kr <sup>34+</sup>	-1.686E+06	-2.180E+05	-3.829E+03	-1.697E+06	1.805E+05	-3.828E+03
Rb <sup>35+</sup>	-1.781E+06	-2.233E+05	-4.369E+03	-1.793E+06	1.847E+05	-4.369E+03
Sr <sup>36+</sup>	-1.879E+06	-2.285E+05	-4.970E+03	-1.892E+06	1.889E+05	-4.971E+03
Y <sup>37+</sup>	-1.979E+06	-2.337E+05	-5.644E+03	-1.994E+06	1.931E+05	-5.646E+03
Zr <sup>38+</sup>	-2.082E+06	-2.390E+05	-6.394E+03	-2.099E+06	1.974E+05	-6.397E+03
Nb <sup>39+</sup>	-2.188E+06	-2.443E+05	-7.227E+03	-2.206E+06	2.018E+05	-7.233E+03
Mo <sup>40+</sup>	-2.296E+06	-2.497E+05	-8.151E+03	-2.315E+06	2.063E+05	-8.159E+03
Tc <sup>41+</sup>	-2.406E+06	-2.551E+05	-9.179E+03	-2.427E+06	2.109E+05	-9.190E+03
Ru <sup>42+</sup>	-2.518E+06	-2.614E+05	-1.031E+04	-2.542E+06	2.164E+05	-1.033E+04
Rh <sup>43+</sup>	-2.634E+06	-2.663E+05	-1.158E+04	-2.659E+06	2.204E+05	-1.160E+04
Pd <sup>44+</sup>	-2.751E+06	-2.719E+05	-1.297E+04	-2.779E+06	2.253E+05	-1.299E+04
Ag <sup>45+</sup>	-2.871E+06	-2.777E+05	-1.451E+04	-2.902E+06	2.304E+05	-1.454E+04
Cd <sup>46+</sup>	-2.993E+06	-2.835E+05	-1.620E+04	-3.026E+06	2.357E+05	-1.624E+04
In <sup>47+</sup>	-3.117E+06	-2.894E+05	-1.808E+04	-3.154E+06	2.411E+05	-1.812E+04
Sn <sup>48+</sup>	-3.244E+06	-2.954E+05	-2.013E+04	-3.283E+06	2.467E+05	-2.018E+04
Sb <sup>49+</sup>	-3.373E+06	-3.014E+05	-2.241E+04	-3.416E+06	2.524E+05	-2.247E+04
Te <sup>50+</sup>	-3.504E+06	-3.075E+05	-2.488E+04	-3.550E+06	2.583E+05	-2.495E+04
I <sup>51+</sup>	-3.637E+06	-3.136E+05	-2.767E+04	-3.687E+06	2.644E+05	-2.776E+04
Xe <sup>52+</sup>	-3.773E+06	-3.198E+05	-3.068E+04	-3.827E+06	2.707E+05	-3.079E+04
Cs <sup>53+</sup>	-3.910E+06	-3.259E+05	-3.402E+04	-3.968E+06	2.771E+05	-3.414E+04
Ba <sup>54+</sup>	-4.049E+06	-3.321E+05	-3.765E+04	-4.112E+06	2.837E+05	-3.780E+04
La <sup>55+</sup>	-4.191E+06	-3.382E+05	-4.168E+04	-4.258E+06	2.904E+05	-4.185E+04
Ce <sup>56+</sup>	-4.334E+06	-3.443E+05	-4.611E+04	-4.406E+06	2.974E+05	-4.631E+04
Pr <sup>57+</sup>	-4.479E+06	-3.504E+05	-5.098E+04	-4.557E+06	3.045E+05	-5.122E+04
Nd <sup>58+</sup>	-4.626E+06	-3.563E+05	-5.628E+04	-4.709E+06	3.118E+05	-5.656E+04
Pm <sup>59+</sup>	-4.775E+06	-3.622E+05	-6.214E+04	-4.864E+06	3.193E+05	-6.246E+04
Sm <sup>60+</sup>	-4.925E+06	-3.680E+05	-6.844E+04	-5.020E+06	3.270E+05	-6.882E+04
Eu <sup>61+</sup>	-5.076E+06	-3.736E+05	-7.545E+04	-5.178E+06	3.348E+05	-7.588E+04
Gd <sup>62+</sup>	-5.229E+06	-3.790E+05	-8.300E+04	-5.338E+06	3.429E+05	-8.350E+04
Tb <sup>63+</sup>	-5.383E+06	-3.842E+05	-9.139E+04	-5.499E+06	3.512E+05	-9.197E+04
Dy <sup>64+</sup>	-5.538E+06	-3.892E+05	-1.005E+05	-5.662E+06	3.597E+05	-1.011E+05
Ho <sup>65+</sup>	-5.694E+06	-3.939E+05	-1.105E+05	-5.827E+06	3.683E+05	-1.113E+05
Er <sup>66+</sup>	-5.851E+06	-3.983E+05	-1.215E+05	-5.992E+06	3.772E+05	-1.224E+05
Tm <sup>67+</sup>	-6.009E+06	-4.024E+05	-1.336E+05	-6.159E+06	3.864E+05	-1.346E+05
Yb <sup>68+</sup>	-6.167E+06	-4.060E+05	-1.466E+05	-6.326E+06	3.957E+05	-1.478E+05
Lu <sup>69+</sup>	-6.326E+06	-4.093E+05	-1.610E+05	-6.495E+06	4.053E+05	-1.624E+05
Hf <sup>70+</sup>	-6.484E+06	-4.120E+05	-1.767E+05	-6.664E+06	4.152E+05	-1.782E+05

(continued on next page)

**Table 2 (continued).**

Ta <sup>71+</sup>	-6.642E+06	-4.142E+05	-1.938E+05	-6.833E+06	4.253E+05	-1.956E+05
W <sup>72+</sup>	-6.800E+06	-4.158E+05	-2.125E+05	-7.002E+06	4.357E+05	-2.146E+05
Re <sup>73+</sup>	-6.957E+06	-4.167E+05	-2.331E+05	-7.171E+06	4.464E+05	-2.355E+05
Os <sup>74+</sup>	-7.113E+06	-4.168E+05	-2.553E+05	-7.339E+06	4.575E+05	-2.581E+05
Ir <sup>75+</sup>	-7.267E+06	-4.173E+05	-2.800E+05	-7.506E+06	4.677E+05	-2.831E+05
Pt <sup>76+</sup>	-7.420E+06	-4.165E+05	-3.067E+05	-7.672E+06	4.787E+05	-3.103E+05
Au <sup>77+</sup>	-7.570E+06	-4.151E+05	-3.362E+05	-7.837E+06	4.898E+05	-3.402E+05
Hg <sup>78+</sup>	-7.717E+06	-4.132E+05	-3.679E+05	-7.999E+06	5.006E+05	-3.726E+05
Tl <sup>79+</sup>	-7.861E+06	-4.112E+05	-4.028E+05	-8.158E+06	5.108E+05	-4.082E+05
Pb <sup>80+</sup>	-8.002E+06	-3.869E+05	-4.411E+05	-8.315E+06	5.425E+05	-4.472E+05
Bi <sup>81+</sup>	-8.137E+06	-4.098E+05	-4.831E+05	-8.467E+06	5.261E+05	-4.900E+05

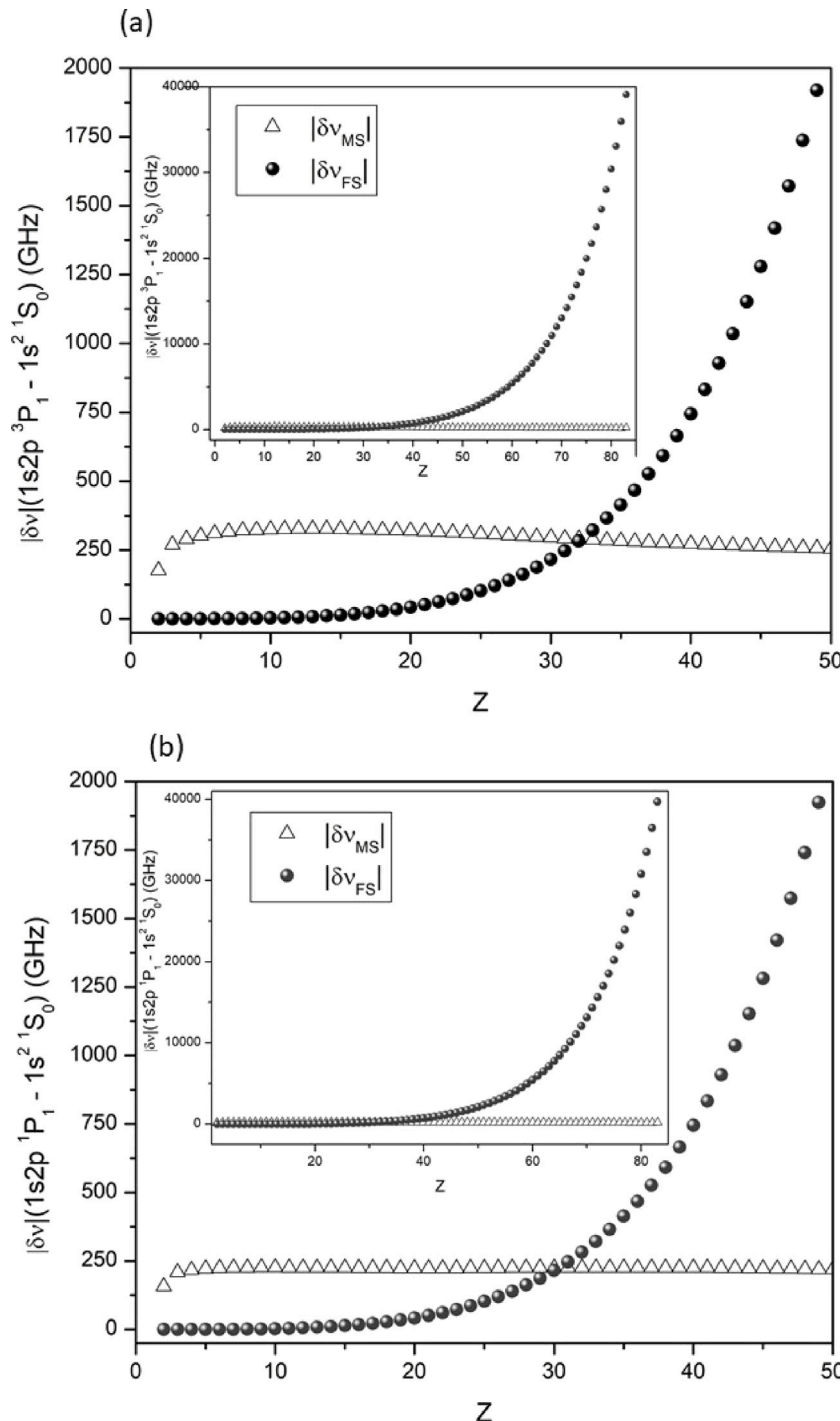


**Fig. 4.** Absolute value of the mass shifts  $|\delta v_{MS}|$  and field shifts  $|\delta v_{FS}|$  as functions of the nuclear charge  $2 \leq Z \leq 83$ . All values in GHz, for  $1s^2 \ ^1S_0 - 1s2p \ ^1,3P_1^o$  transitions calculated for the isotope pair (A, A + 1).

considerably increased towards high-Z values and become dominant at the end of the sequence. By way of illustration, the field shift is one order of magnitude larger than the mass shift for the He-like ions. As a result, one can neglect the mass shift for  $60 \leq Z$  ions. Besides, it should be underlined that the field and mass shifts have opposite signs and, therefore, cancel out around  $Z = 33$  ( $As^{32+}$ ) given rise to a total isotope shift close to zero.

## 5. Outlook and conclusion

In this work, we present calculations of the isotope shifts of four transitions between the complex  $n = 1$  and  $n = 2$  in helium-like ions of nuclear charge numbers  $Z = 2 - 83$ . Relativistic and correlation contributions to the field and mass shifts, along with the corresponding QED effects are included. The effects of nuclear polarization and deformation are also taken into account. The electronic isotope shift parameters: the normal mass shift, specific mass shift, isotope shift and field shift parameters, are calculated using the fully relativistic MCDHF/RCI method and RIS4 module. It is found that the NMS and SMS parameters of  $1s^2 {}^1S_0 - 1s 2p {}^3P_{0,2}^o$  and the  $1s^2 {}^1S_0 - 1s 2p {}^3,1P_1^o$  transitions change nonmonotonically along the He-like isoelectronic sequence. Comparisons are made with the mass- and field-shifts by Zubova et al. [11] for the isotope pair of He-like Mg, Ca, Zn, Zr, Sn, Nd Yb, and Hg ions. Except for the FS of the heavy elements where the discrepancies can reach up to  $\sim 40\%$ , they show a good agreement with our MCDHF/RCI predictions.. We can conclude that for highly charged ions, field shifts affects more the transition lines than the mass shifts MS.

## CRediT authorship contribution statement

**Sirine Ben Nasr:** Conceptualization, Data curation, Formal analysis, Methodology, Writing – original draft. **Soumaya Manai:** Conceptualization, Data curation, Methodology. **Dhia Elhak Salhi:** Conceptualization, Data curation, Methodology. **Haikel Jelassi:** Data curation, Formal analysis, Supervision, Writing – original draft, Writing – review & editing.

## Declaration of competing interest

The authors declare that they have no known competing financial interests or personal relationships that could have appeared to influence the work reported in this paper.

## Data availability

No data was used for the research described in the article.

## Acknowledgments

The authors would like to acknowledge the financial support of the Tunisian Ministry of Higher Education and Scientific Research. The authors are also grateful for the financial support from International Atomic Energy Agency, Austria, research project contract: IAEA CRP F43026, “Atomic Data for Injected Impurities in Fusion Plasmas”.

## References

- [1] Sanchez, et al. Phys Rev Lett 2006;96:033002.
- [2] Cheal B, et al. Phys Rev Lett 2010;104:252502.
- [3] Charlwood FC, et al. Phys Lett B 2010;690:346.
- [4] Lundqvist M, et al. Astron Astrophys 2007;463:693.
- [5] Roederer IU, et al. Astrophys J Suppl Ser 2012;203:27.
- [6] Kasen D, et al. Nature 2017;551:80.
- [7] Blondel C, Delsart C, Valli C, Yiou S, Godefroid MR, Van Eck S. Phys Rev A 2001;64:052504.
- [8] Carette T, Godefroid MR. Phys Rev A 2011;83:062505.
- [9] Carette T, Godefroid MR. J Phys B 2011;44:105001.
- [10] Shabaev VM, et al. J Phys B 1998;31:L337.
- [11] Zubova NA, et al. Opt Spectrosc 2020;128:1090–9.
- [12] Zubova NA, et al. Phys Rev A 2014;90:062512.
- [13] Zubova NA, et al. Phys Rev A 2016;93:052502.
- [14] Grant IP. Relativistic Quantum Theory of Atoms and Molecules. New York: Springer, 2007.
- [15] Froese Fischer C, Gaigalas G, Jönsson P, Bieroń J. Comput Phys Commun 2019;237:184–7.
- [16] Ekman J, Jönsson P, Godefroid M, Naze C, Gaigalas G, Bieroń J. Comput Phys Commun 2019;235:433–46.
- [17] Jönsson P, Gaigalas G, Bieroń J, Froese Fischer C, Grant IP. Comput Phys Commun 2013;184:2197.
- [18] Dyal KG, Grant IP, Jönsson CT, Parpia FA, Plummer PE. Comput Phys Commun 1989;55:425.
- [19] Blundell SA, Baird PEG, Palmer CWP, Stacey DN, Woodgate GK. J Phys B: At Mol Phys 1987;20:3663.
- [20] Parpia FA, Mohanty AK. Phys Rev A 1992;46:3735.
- [21] Torbohm G, Fricke B, A. Rosén A. Phys Rev A 1985;31:2038.
- [22] Li JG, Nazé C, Godefroid M, Fritzsche S, Gaigalas G, Indelicato P, Jönsson P. Phys Rev A 2012;86:022518.
- [23] Seltzer EC. Phys Rev 1969;188:1916.
- [24] Schiopet R, Harman Z, Scheid W, N Grün. Eur Phys J D 2004;21:31.
- [25] Andrae D. Phys Rep 2000;336:413.
- [26] Palmer CWP. J Phys B: At Mol Phys 1987;20:5987.
- [27] Gaidamauskas E, Nazé C, Rynkun P, Gaigalas G, Jönsson P, Gaigalas G. J Phys B: At Mol Opt Phys 2011;44:175003.